scientific reports

Check for updates

OPEN

Intramuscular neural distribution of the vastus lateralis informs effective and safe botulinum neurotoxin injection

Kyu-Ho Yi[1,2,6], Hyewon Hu[1,6], Sung-Oh Hwang[3], Ji-Hyun Lee[4]✉ & Hyung-Jin Lee[5]✉

Understanding the nerve distribution within the vastus lateralis muscle in relation to anatomical landmarks is essential for effective botulinum neurotoxin injections to manage chronic anterior knee pain and vastus lateralis muscle tone disorders. This study proposes an anatomically informed approach for administering these injections to the vastus lateralis muscle. Using a modified Sihler's method, we examined nerve distribution in the vastus lateralis muscles of 12 fresh cadavers. The muscles were analyzed with respect to a transverse line crossing the greater trochanter of the femur and the base of the patella, dividing them into four zones from top to bottom. Ultrasonography was used to examine the muscle anatomy and to guide injections, confirming both structural details and injection accuracy. Intramuscular nerve distribution in the vastus lateralis muscle showed significant patterns, particularly in zones 2 and 3. Based on the nerve distribution and surface landmarks, ultrasonography-guided injections showed high accuracy without damage to surrounding essential anatomical structures. Targeting botulinum neurotoxin injections at the areas with the densest nerve distribution is recommended. Adhering to these guidelines enables clinicians to use minimal doses and reduce the risk of adverse effects such as gait disturbances, antibody production, and bruising from multiple injections.

Keywords Clinical guideline, Vastus lateralis, Chronic anterior knee pain, Spasticity, Botulinum neurotoxin

The vastus lateralis (VL), which is the largest component of the quadriceps femoris muscle group, plays a critical role in knee extension and stabilization[1]. Appropriate VL function is essential for activities, such as walking, running, and squatting[2]. Dysfunction of the VL has been implicated in various clinical conditions, including chronic anterior knee pain (AKP) and muscle spasticity[3].

AKP is a broad term encompassing anterior knee pain conditions, incl[2]uding patellofemoral pain syndrome (PFPS), and is known to significantly impair lower limb function and reduce quality of life[4]. Anatomically, AKP frequently results from altered joint mechanics between the patella and femur, commonly caused by abnormal activation patterns within the quadriceps, particularly between the vastus medialis (VM) and VL[3,5]. However, decreased VM activity and relatively increased VL activation can cause lateral displacement of the patella, increased patellofemoral joint pressure, subsequent microcartilage damage, and localized anterior knee pain[5–8].

Management of AKP varies depending on the underlying cause and includes VM-strengthening exercise therapy, neuromuscular electrical stimulation, and botulinum neurotoxin type A (BoNT-A)[6,9,10]. Among these, BoNT-A has gained increasing attention as a selective intervention for reducing the lateral patellar pull caused by excessive VL activity[8,10]. BoNT-A injections into the VL inhibit acetylcholine release at the neuromuscular junction, temporarily decreasing muscle tone and promoting functional rebalancing between the hyperactive VL and underactive VM[11,12]. This, in turn, facilitates patellar recentering and may alleviate symptoms in patients with chronic AKP who are unresponsive to conservative treatment.

[1]Division in Anatomy and Developmental Biology, Department of Oral Biology, BK21 PLUS Project, Human Identification Research Institute, Yonsei University College of Dentistry, 50-1 Yonsei-ro, Seoul 03722, Republic of Korea. [2]You and I Clinic, Seoul, Republic of Korea. [3]Thank You Plastic Surgery Clinic, Seoul, Republic of Korea. [4]Department of Anatomy and Acupoint, College of Korean Medicine, Gachon University, Seongnam 13120, Republic of Korea. [5]Department of Anatomy, College of Medicine, Chungbuk National University, Chungdae-ro 1, Seowon-gu, Cheongju, Chungbuk 28644, Republic of Korea. [6]Kyu-Ho Yi and Hyewon Hu contributed equally to this work. ✉email: anatomy@gachon.ac.kr; leehj@cbnu.ac.kr

VL spasticity may also cause functional impairment owing to hypertonicity or overactivation. As part of the upper motor neuron syndrome, spasticity frequently follows neurological injuries, such as stroke, cerebral palsy, or multiple sclerosis. Spasticity is characterized by hyperactive stretch reflexes and exaggerated tendon reflexes owing to reduced central inhibition[13,14]. Given the strong extensor moment of the knee joint, excessive VL spasticity may restrict knee flexion and induce genu recurvatum. Prolonged knee hyperextension may further result in gait abnormalities, pain, and posterior capsular injury[15,16]. General treatment options include physical therapy, phenol or BoNT-A injections, or surgical interventions. Among these, BoNT-A serves as an effective adjunct therapy for controlling spasticity[17,18].

Previous studies have reported that a combination of BoNT-A injections into the VL and physical therapy is effective in treating both AKP and spasticity[3,4,8,10]. Thus, BoNT-A injection into the VL may serve as a targeted and efficient therapeutic strategy to restore functional balance and improve clinical outcomes. BoNT-A efficacy relies heavily on the precise targeting of presynaptic nerve terminals near the motor endplate, particularly within intramuscular neural arborization zones. Clinical trials have demonstrated that targeting these neural zones in muscles results in greater muscle volume reduction than non-targeted injections[19,20].

Given the large size and complex intramuscular innervation of the VL, appropriate dosing and accurate targeting are essential for optimizing BoNT-A injection efficacy. Anatomical studies have shown that the VL is innervated by the femoral nerve, with the densest innervation in its proximal and mid-regions, making these areas ideal targets for BoNT-A administration[21,22]. More recent studies have gone beyond general innervation patterns to map fine intramuscular neural arborizations[23].

In this study, we employed Sihler's whole-mount nerve staining technique, which enables the visualization of fine intramuscular neural branches without causing tissue damage, to map the detailed intramuscular innervation pattern of the VL. Based on this, we aimed to provide precise anatomical information to support safe and effective administration of BoNT-A targeting the VL.

Materials and methods

Approvement of the study

This study adhered to the ethical principles outlined in the Declaration of Helsinki. All cadavers were lawfully donated to the Catholic University of Korea with prior approval from the Institutional Review Board (IRB No. MC23EISE0022). The families of the cadavers provided explicit consent for the dissection procedures.

Procurement of the specimen and gross anatomy

Twelve fresh adult Korean cadavers (seven males and five females; mean age at death: 82.7 years; range: 67–89 years) were used. All twelve were used to investigate the femoral nerve entry points and intramuscular nerve distribution patterns, whereas two cadavers were additionally used to evaluate ultrasound-guided injection procedures.

The anterior thigh region, including the skin, subcutaneous tissue, and fascia lata, was carefully dissected to expose the branches of the femoral nerve. Two sequential analyses were conducted to confirm the distribution patterns of the VL.

Number of femoral nerve branches and their entry points into the VL

To identify the origin of the nerves innervating the VL, a meticulous dissection was performed to avoid nerve damage. The VL was separated from the femur and from the greater trochanter up to the superior border of the patella. The muscle was divided into four equal sections along its longitudinal length, labeled as zones 1, 2, 3, and 4. The following parameters were recorded: (1) the number of branches arising from the femoral nerve innervating the VL and (2) the number and location of entry points of these branches into each muscle section.

Intramuscular nerve distribution patterns of the VL: modified sihler's staining

After detaching the VL from the femur and patella, modified Sihler's staining was used to visualize the intramuscular nerve branching patterns. This protocol differs from traditional methods[24]. Throughout the procedure, the processing time was adjusted based on muscle thickness and staining intensity, ensuring optimal results rather than adhering to a fixed duration. The detailed staining steps and chemical agents used are as follows:

Fixation Muscles were fixed in 10% unneutralized formaldehyde for seven days.

Maceration and depigmentation The fixed specimens were macerated and depigmented over 2–3 weeks using a 3% aqueous potassium hydroxide solution supplemented with 1 mL of 3% hydrogen peroxide per 1000 mL. To accelerate the maceration, the muscles were carefully agitated and gently compressed at regular intervals.

Decalcification and whitening Following maceration, the specimens were decalcified and whitened using a three-day "Sihler I solution," which comprises a mixture of 10% glacial acetic acid and 10% glycerin in distilled water.

Staining Post-decalcification, the specimens underwent staining in "Sihler II solution," composed of 10% Ehrlich's hematoxylin and 10% glycerin in distilled water, for 3–4 days.

Destaining The stained specimens were then destained using Sihler I solution for 3–7 h. To accelerate the destaining reaction, the muscles were carefully agitated and gently compressed at regular intervals.

Neutralization and blueing After destaining, the specimens were neutralized under running tap water for 1 h and then immersed in 0.05% lithium carbonate for an additional hour to facilitate the blueing of the nerve fibers.

Clearing Finally, the neutralized samples were cleared to enhance their transparency. Although both formamide and glycerin are viable clearing agents, 99% formamide was selected due to its faster processing time.

The stained samples were examined using a medical film viewer (light box) that provided sufficient illumination to visualize the intramuscular course of the nerve branches. The intramuscular distribution patterns within the VL were analyzed using direct visual inspection, hand-drawn sketches, written observations, and photographic documentation.

The entry points and distribution patterns of the nerves were thoroughly examined. The VL was vertically divided into four equal-length zones between the reference points of the greater trochanter of the femur and the base of the patella. Each zone represented 25% of the total length and was labeled as zones 1, 2, 3, and 4. In each section, a 3× dissecting microscope was used to trace the nerves to their terminal branches until they were no longer visible. The number of these terminal nerve endings was recorded, and the total number of innervated samples was analyzed and quantified for each section. Nerve density was calculated as follows: In stained and four-sectioned VL specimens, three authors independently counted nerve endings in each section (zones 1–4) under a 3× dissecting microscope, and the counts were cross-verified. Based on this detailed analysis, the zones of the VL with the highest frequency of nerve entries and the densest intramuscular nerve distribution were identified.

Ultrasonography examination and ultrasound-guided injection procedure

Based on the results of this study, an ultrasound-guided injection was performed using four thigh sides from two fresh cadavers. Real-time B-mode ultrasonography was performed using an HS50 system (Samsung, Seoul, Republic of Korea) equipped with a linear transducer (LA3-14AD; 3–14 MHz). Surface landmarks, including the greater trochanter of the femur and the base of the patella (BoP), were first located by palpation and marked on the cadaver's skin with a permanent surgical pen, dividing the thigh into four zones. Based on these four zones, the skin, subcutaneous tissue, and muscle thickness was measured before the ultrasound-guided injection into the VL.

Ultrasonography was performed on unfixed cadavers. A generous amount of ultrasound gel was applied to minimize compression of the skin and underlying structures, as excessive pressure on the tissue surface reduces image quality. The probe was positioned as perpendicular as possible to both the skin and the underlying bone at the target anatomical region. Ultrasound settings were adjusted according to the condition of the cadaver, with particular optimization of gain and grayscale levels until the clearest image was obtained. Scanning depth was set between 3 and 5 cm, depending on muscle thickness, and the highest available frequency was used to maximize resolution.

During the scanning process, the ultrasonography transducer was placed transversely to differentiate between the vastus intermedius and VL (Fig. 1). Subsequently, the transducer was shifted towards the VL insertion site to observe whether the muscle gradually narrowed and became thinner. This step confirmed the precise identification of the VL using ultrasonography. Subsequently, both the median and lateral lines of the thigh were trisected, and the injection point was designated as the 2/3 lateral line intersecting the midpoint of the VL (GT to BoP). The transducer was placed close to the puncture site, and the needle was advanced under direct echographic visualization using a real-time technique in the in-plane method, moving transversely.

The injection depth was set to penetrate the skin, subcutaneous tissue, and fascia, because these structures vary in thickness among individuals. After determining the target depth under ultrasound guidance, a 2.54-cm 23-G needle was used to inject the most arborized intramuscular nerve areas. The injections delivered 2 ml of blue dye, with consistent techniques applied bilaterally across all four thighs. After ultrasound-guided injections, each specimen was dissected to confirm appropriate dye targeting of the neural arborized regions. The accuracy of the injections and any complications, defined as unintended needle passage through significant neurovascular structures, were evaluated post-dissection.

Results

The number of femoral nerve branches and the location of their entry points into the VL

The femoral nerve (FN) was divided into two primary branches in most cases (83.3%) and was distributed to the VL (Table 1). The first primary branch (primary-superior branch) innervated the proximal 1/4 region of the VL in all cases except one. It was further divided into two to three smaller branches before being distributed within the VL. The second primary branch (primary-inferior branch) was also divided into smaller branches and innervated the remaining 2/4–3/4 segments of the VL (Fig. 2). None of the cases had a nerve entry point in the 4/4 region of the VL (Table 2).

.

Intramuscular nerve distribution patterns of the VL

The results of Sihler's staining, which was conducted to investigate the fine nerve distribution of the VL, revealed that nerve endings were distributed throughout the entire muscle (Fig. 3). The density of nerve endings per specimen was densest in zone 3 of the VL, reaching 40.4%, whereas zone 1 exhibited the lowest density at 14.1%. The nerves distributed on the medial side of the 1/4 region were primarily derived from the superior primary branch of the FN, whereas the remaining regions were innervated by smaller branches of the inferior primary branch (Table 3).

The nerve is distributed throughout the muscle but is most prominently concentrated in zone 3 (between 2/4 and 3/4). (The red circles indicate the locations of nerve endings.)

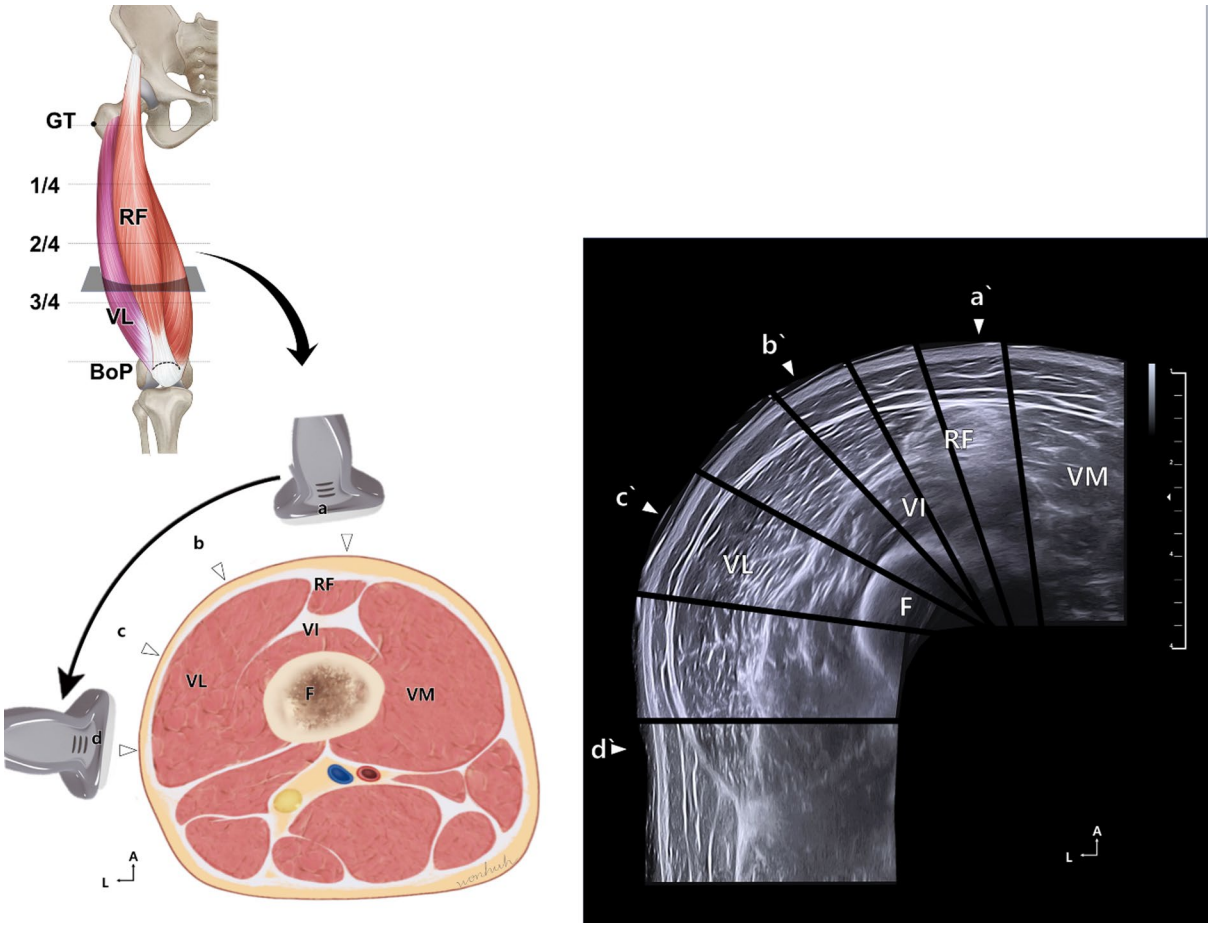

Fig. 1. Ultrasonography scanning method for ultrasound-guided injections and corresponding cross-sectional images. Three transverse lines (1/4, 2/4, and 3/4) divided the vastus lateralis (VL) into four zones. The black transparent plane in the upper left illustration represents the scanning site. Scanning was performed from points a to d in the anterior-to-lateral direction to visualize the entire VL muscle, with each site corresponding to a′–d′ in the ultrasonography image. GT, greater trochanter; BoP, base of patella; RF, rectus femoris muscle; VI, vastus intermedius; VM, vastus medialis; F, femur; A, anterior; L, lateral.

Number	1	2	3
Frequency	8.3%	83.3%	8.3%

Table 1. Number of nerve branches of the FN distributed to the VL.

The thickness of the skin, fat, and muscle

In a separate experiment, we measured the thickness of the VL in two cadavers using ultrasonography (Fig. 4). The thicknesses of the skin, subcutaneous fat, and muscle were assessed across zones 2–4 of the VL. The data revealed distinct trends in the thickness of each layer, as detailed in Table 4.

Skin thickness remained relatively constant across zones 2–4. Although fat thickness exhibited slight fluctuations, it showed an overall consistency within the same zones. In contrast, muscle thickness increased progressively from zone 2 to zone 3, and then decreased in zone 4.

Injection accuracy of ultrasound-guided injection into the area with the densest nerve termination density

The accuracy of ultrasound-guided injections was assessed according to the area with the densest nerve termination of the VL and surface landmarks. Specifically, the injections were targeted at the midpoint of the VL. Although the injection volume was only 2 ml, the dye spread along the muscle fibers to a distance of approximately 15 cm and was widely distributed in zones 2–4. (Fig. 5). Complete insertion of the standard needle was sufficient to reach the target depth. No incorrect injections were administered into the surrounding muscles, such as the vastus intermedius, rectus femoris, or tensor fascia lata. In all cases, the dye was accurately injected into the VL.

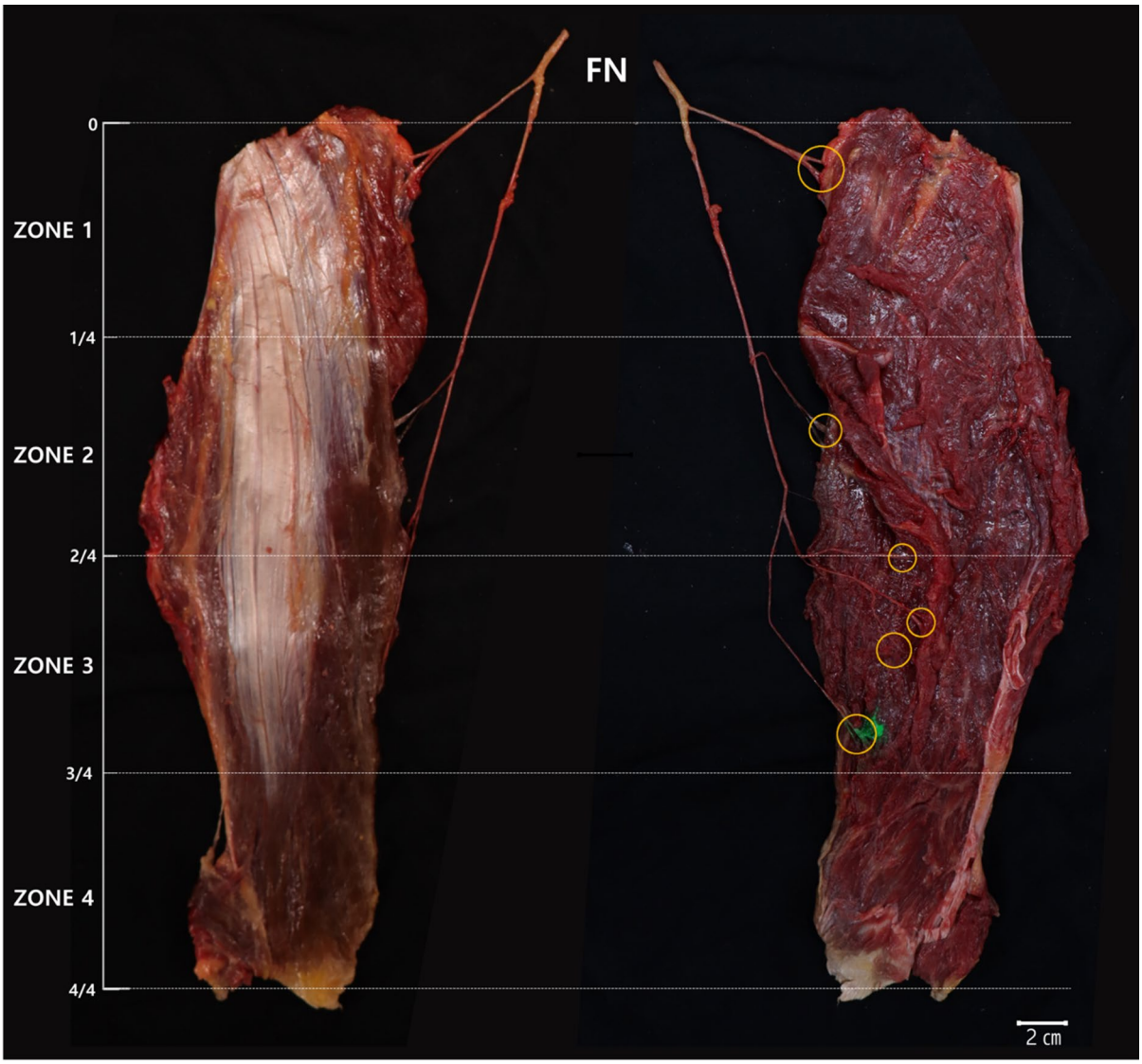

Fig. 2. Femoral nerve (FN) innervation of the vastus lateralis (VL). The image shows the anterior and posterior aspect of a single specimen, with the VL divided into four zones (Zones 1–4) to identify the nerve entry points. The ant. view shows the anterior view of the VL with the nerve branches, while the right specimen shows the posterior view of the muscle, directly displaying the nerve entry points into the VL. Yellow circles indicate the entry points. FN, femoral nerve.

Number of nerve branches	0 (%)	1 (%)	2 (%)	3 (%)	4 (%)
Zone 1	8.3	25.0	41.7	25.0	0.0
Zone 2	16.7	25.0	33.3	8.3	16.7
Zone 3	16.7	25.0	16.7	25.0	16.7
Zone 4	100.0	0.0	0.0	0.0	0.0

Table 2. Frequency of entry points of small nerve branches into distinct zones of VL.

The injection point was located at the midpoint (2/4) between the greater trochanter of the femur (GT) and the base of the patella (BoP). In the right image, the injected dye is observed to have spread extensively along the direction of the muscle fibers, indicating a broad intramuscular dispersion.

Discussion

The present study confirmed that the femoral nerve typically supplies the VL muscle via one to three branches, with most cadavers showing two branches from the femoral nerve trunk dividing into multiple smaller

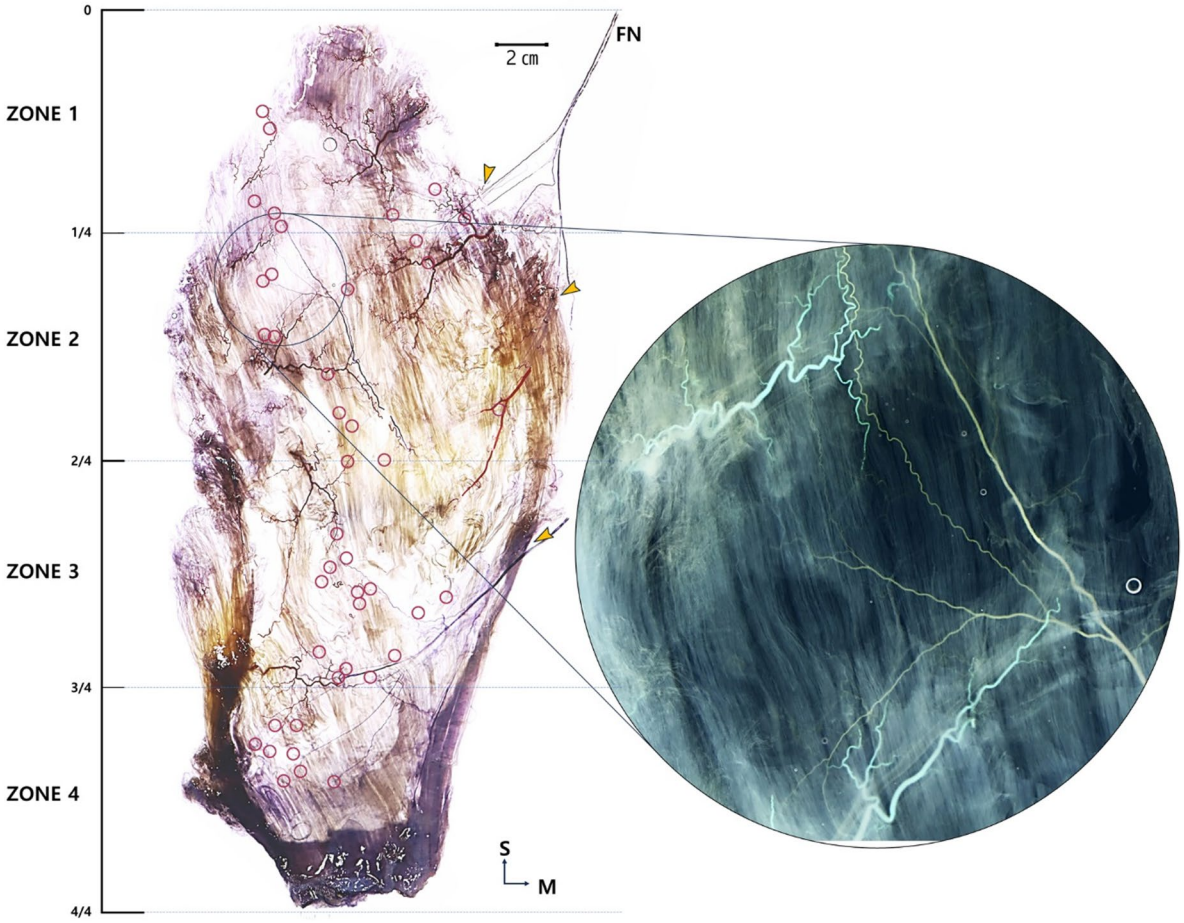

Fig. 3. Distribution Pattern of the femoral nerve (FN) Observed with Sihler's Staining in the vastus lateralis (VL). The enlarged image on the right shows a region of Zone 2 of the VL, illustrating the nerve density within the muscle. Orange arrowheads indicate the nerve entry points into the VL at Zones 1–3. S, superior; M, medial.

Zone (Segment)	1	2	3	4
Average	4.0 ± 2.4 (14.1 ± 5.6)	8.2 ± 6.2 (26.6 ± 14.1)	11.17 ± 3.0 (40.4 ± 8.3)	5.3 ± 3.2 (19.0 ± 12.9)
Range	2–8	2–19	7–15	2–10

Table 3. Frequency of nerve ending distribution by VL region unit: number (percentile).

branches[25,26]. The results of the present study is similar to the previous studies that described the distribution pattern of the femoral nerve branches to the VL muscle[27,28]. Moreover, in terms of entry points, in the present study, the femoral nerve entered the anterior aspect of the VL, particularly Zones 1, 2, and 3, consistent with Patil et al.'s description of the nerve running from anteroproximal to posterodistal within the muscle[22].

In this study, we used Sihler's staining to visualize the VL intramuscular nerve distribution pattern, focusing on its arborization pattern. Previous studies have demonstrated that BoNT injections targeting areas of dense intramuscular nerve arborization are more effective[19,20]. Although most skeletal muscles typically exhibit a single nerve entering the center of the muscle with arborization concentrated in the central region, the VL displayed a different pattern. Although the arborization was densest in zone 3, the VL was innervated by multiple nerves due to its large and broad anatomical structure. Consequently, the distribution of nerve endings was more extensive across the muscle. These findings suggest that when targeting the VL for BoNT injections, a broader injection area and carefully adjusted dosages may be necessary to achieve effective outcomes.

To better understand the anatomical variability of the structures in the VL region, ultrasonography was used to assess the detailed thickness of the skin, subcutaneous fat, and muscles along the length of the VL. Although skin thickness remained relatively constant, fat thickness decreased in the mid-thigh region and increased slightly distally. Muscle thickness increased from the proximal to mid-thigh, and then declined significantly in the distal region. These findings align with those of previous reports indicating a greater cross-sectional area

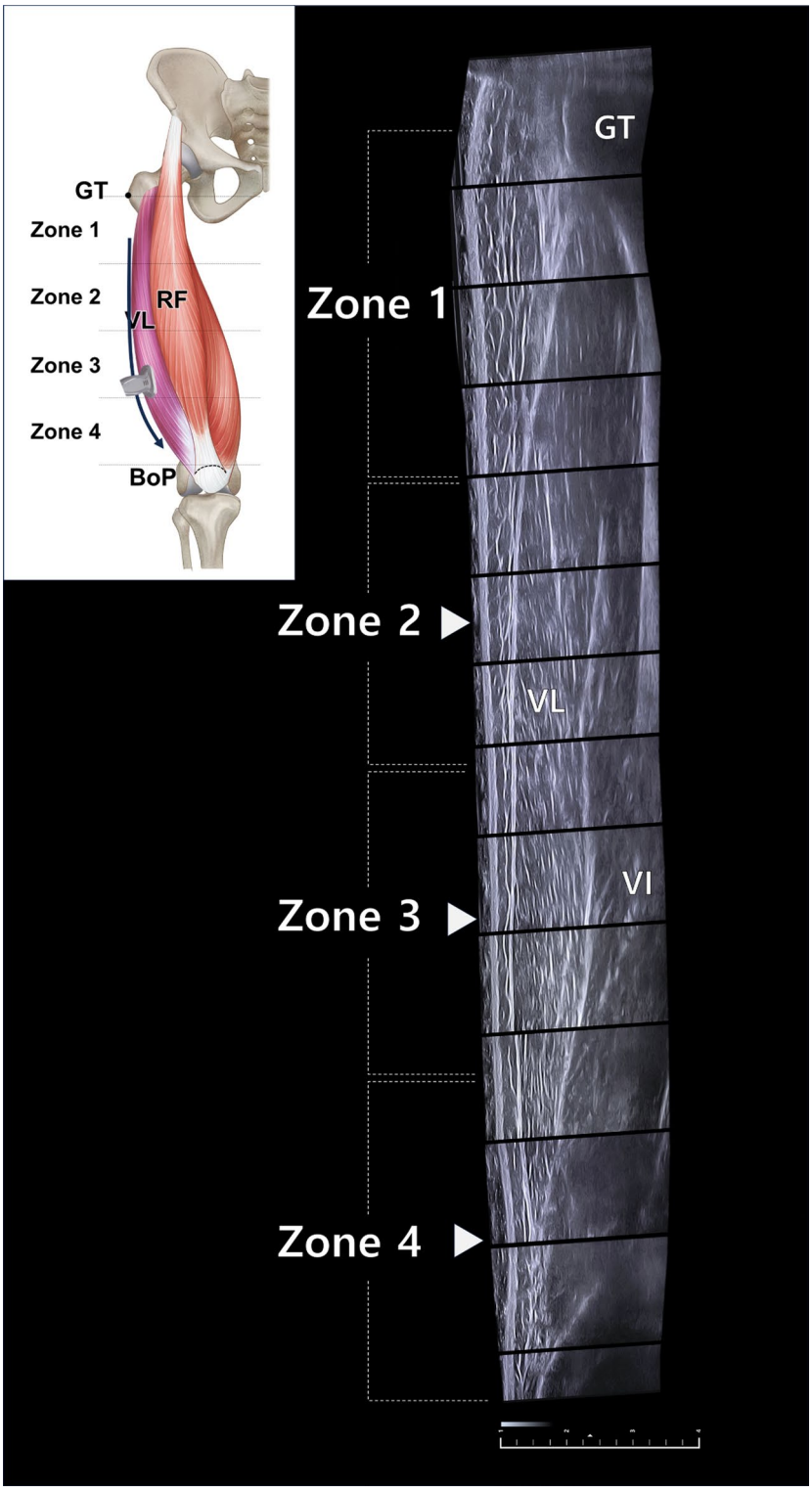

Fig. 4. Panoramic ultrasound image from the greater trochanter to the base of the patella at a 45-degree angle of the thigh. The thickness of the VL was measured in each zone except zone 1. GT, greater trochanter; BoP, base of patella; RF, rectus femoris muscle; VL, vastus lateralis; VI, vastus intermedius.

in the central portion of the VL[29,30]. Moreover, our findings showed that the muscle was the thickest in zone 3, which is consistent with the anatomical mid-region of the VL. However, the overall muscle thickness in our study was notably lower than that reported in previous studies, likely due to age-related muscle atrophy in elderly specimens[31,32]. Therefore, these thickness measurements may not fully reflect those of living individuals and

Zones	Skin (SD)	Fat (SD)	Unit: mm Muscle (SD)
2	1.4 ± 0.3	2.4 ± 1.6	5.7 ± 2.7
3	1.4 ± 0.3	1.8 ± 1.5	6.7 ± 3.3
4	1.3 ± 0.4	2.2 ± 1.7	3.3 ± 1.6

Table 4. Detailed thickness measurements of the skin, fat, and muscle across different thigh regions. SD, standard deviation.

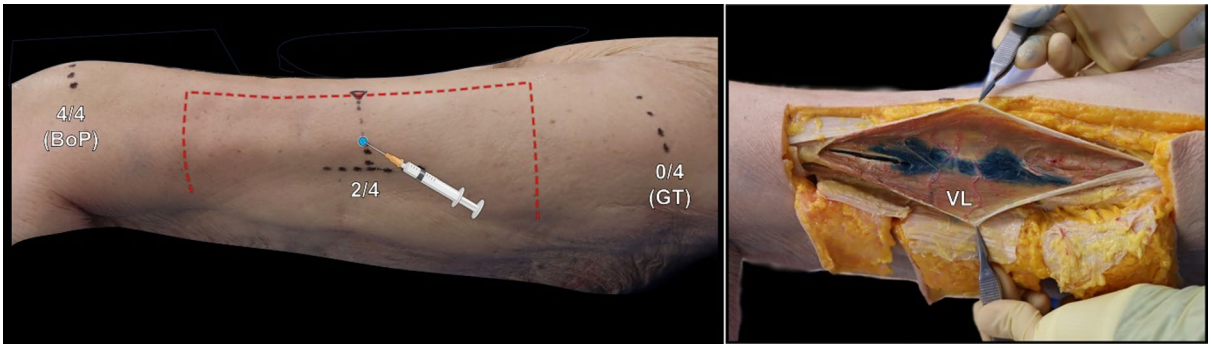

Fig. 5. Cadaveric image of the lateral thigh region following an ultrasound-guided injection targeting the vastus lateralis (VL) muscle. The left panel shows the injection site determined by surface landmarks, including the greater trochanter (GT) and base of patella (BOP). The right panel illustrates the injection outcome, with the dye confined to the VL and distributed along the muscle fibers.

should be interpreted cautiously. Despite this limitation, the observed variability highlights the importance of using ultrasonography to guide BoNT injections, particularly in older populations.

In addition to data on the thickness of the skin, subcutaneous fat, and muscles, we evaluated and established an ultrasound-guided injection strategy using practical surface landmarks. This reduces the risk of misdirected injections, which can lead to functional loss or mobility impairment[33]. This is particularly important in older individuals who are more prone to muscle weakness and imbalance. Our ultrasound-guided injection results confirmed that the injected dye remained localized within the VL area without diffusing into adjacent muscle structures. Thus, the precise application of BoNTs using ultrasonography is critical for preventing the side effects of BoNT injection and optimizing the injection results. This highlights the precision and clinical utility of the proposed injection site and surface landmark methods. Individual variability in fat and muscle thickness is essential, and the needle length should be adjusted accordingly to ensure accuracy.

Previous randomized controlled studies that investigated BoNT injections for anterior knee pain and patellofemoral dysfunction support these clinical implications[3]. BoNT-A injections significantly improved the anterior knee pain scale scores and reduced pain during kneeling, squatting, and walking. Pal et al. further explored the effects of BoNT on the VL-VM balance, patellar tracking, and pain in patients with persistent patellofemoral pain[5]. Imaging confirmed improvements in patellar tracking metrics and pain reduction immediately after the intervention, with effects lasting up to two years. These studies support the efficacy of BoNT injections combined with rehabilitation and validate the rationale behind targeted injection strategies.

BoNTs are typically administered near neuromuscular junctions to inhibit acetylcholine release. Identifying regions with dense motor nerve terminations ensures safer and more effective injections. Only one anatomical study by Li et al. reported nerve-dense regions within the VL, located at the center of the distribution at approximately 48.9% of the muscle length, ranging from 25 to 72%[34]. Our findings align with this, identifying zone 3 as the primary site of dense innervation based on surface landmarks, such as the ASIS and the base of the patella. Palpation of these landmarks can help clinicians localize the optimal injection zone and improve safety and efficacy, particularly in patients with anterior knee or patellofemoral pain.

The traditional BoNT injection site for the VL muscle, aimed at relieving anterior knee pain and patellofemoral pain, has been suggested to be in the distal part of the VL muscle at 3 cm intervals starting 3–5 cm above the patella at an oblique angle just lateral to the midline or at the distal third of the VL muscle[3,8,35]. These injection sites were based on electromyographic signals from patients, and the therapeutic effect of BoNT injections was beneficial for patients with persistent patellofemoral pain. Although an electromyography-based BoNT injection strategy could be an option, without clearly identifying the thickness or positional relationships of the surrounding structures, injections may inevitably be delivered to unintended areas because the needle path or location cannot be accurately monitored. To improve this, we used ultrasonography to measure the thickness of the skin, subcutaneous tissue, and muscles along the VL muscle across different thigh regions to understand the thickness trends and optimize injection accuracy. The skin remained stable across the areas, whereas fat thickness decreased in the middle region and slightly increased at the 9/10 region. Muscle thickness followed

a similar trend, rising from 5/10 to 7/10 (middle region) but significantly decreasing at the 9/10 region (distal region). These findings align with those of previous studies, showing greater cross-sectional area and muscle mass in the mid-region of the VL[21,36,37].

This study has some limitations. First, the sample size was relatively small, and cadaveric models may not fully replicate dynamic physiological conditions. As cadavers were used, we could not assess the in vivo diffusion or pharmacological effects of the injection. Although we confirmed the anatomical accuracy and safety of ultrasound-guided injections, further clinical validation is required. Second, our study focused exclusively on elderly Korean cadavers, which limits the generalizability across age and ethnicity. As the nerve branches of elderly individuals gradually decrease due to reduced motor demands, the current results cannot be directly applied to younger populations. More detailed cadaveric studies or investigations of nerve distribution in younger individuals should be conducted to comprehensively assess age-related nerve distribution and develop effective pain management strategies that involve responses to BoNTs.

Conclusion

Our study provides detailed insights into the intramuscular nerve distribution in the VL and offers a refined injection strategy that incorporates ultrasonography and anatomical landmarks. The densest arborization was observed in zone 3, and ultrasound-guided injections targeting this area were precise and confined to the VL muscle. These findings emphasize the clinical importance of combining imaging guidance with surface anatomy to optimize the accuracy and safety of BoNT injections. However, further clinical validation is required to confirm these benefits in different patient populations.

Data availability

The data are available from the corresponding author upon reasonable request.

Received: 10 September 2024; Accepted: 28 January 2026
Published online: 05 February 2026

References

1. Gray, H. & Standring, S. *Gray's anatomy: The anatomical basis of clinical practice*. XVII, 1588 s.: ill. (Elsevier, 2021).
2. Colyer, S. L. & McGuigan, P. M. Textile electrodes embedded in clothing: A practical alternative to traditional surface electromyography when assessing muscle excitation during functional movements. *J. Sports Sci. Med.* **17**, 101–109 (2018).
3. Singer, B. J., Silbert, P. L., Song, S., Dunne, J. W. & Singer, K. P. Treatment of refractory anterior knee pain using botulinum toxin type A (Dysport) injection to the distal vastus lateralis muscle: A randomised placebo controlled crossover trial. *Br. J. Sports Med.* **45**, 640–645 (2011).
4. Kesary, Y. et al. Botulinum toxin injections as salvage therapy is beneficial for management of patellofemoral pain syndrome. *Knee Surg. Relat. Res.* **33**, 39 (2021).
5. Pal, S. et al. Patellar Tilt correlates with vastus lateralis: Vastus medialis activation ratio in maltracking patellofemoral pain patients. *J. Orthop. Res.* **30**, 927–933 (2012).
6. LaBore, A. J. & Weiss, D. J. Vastus lateralis strain associated with patellofemoral pain syndrome: A report of 2 cases. *Arch. Phys. Med. Rehabil.* **84**, 613–615 (2003).
7. Lin, F. et al. In vivo patellar tracking induced by individual quadriceps components in individuals with patellofemoral pain. *J. Biomech.* **43**, 235–241 (2010).
8. Pal, S., Choi, J. H., Delp, S. L. & Fredericson, M. Botulinum neurotoxin type A improves Vasti muscle balance, patellar tracking, and pain in patients with chronic patellofemoral pain. *J. Orthop. Research®*. **41**, 962–972 (2023).
9. Barton, C. J., Lack, S., Hemmings, S., Tufail, S. & Morrissey, D. The 'Best practice guide to conservative management of patellofemoral pain': Incorporating level 1 evidence with expert clinical reasoning. *Br. J. Sports Med.* **49**, 923–934 (2015).
10. Tang, A. C. W., Chen, C. K., Wu, S. Y. & Tang, S. F. Improvement of pain and function by using botulinum toxin type A injection in patients with an Osteoarthritic knee with patellar malalignment: An electromyographic study. *Life* **13**, 95 (2022).
11. Collins, N. et al. Foot orthoses and physiotherapy in the treatment of patellofemoral pain syndrome: Randomised clinical trial. *BMJ* **337** (2008).
12. Dressler, D. & Adib Saberi, F. Botulinum toxin: Mechanisms of action. *Eur. Neurol.* **53**, 3–9 (2005).
13. Lance, J., Feldman, R. & Young, R. *Spasticity, disordered motor control* (Chicago Year book Medical, 1980).
14. Pandyan, A. et al. Spasticity: clinical perceptions, neurological realities and meaningful measurement. *Disabil. Rehabil.* **27**, 2–6 (2005).
15. Boudarham, J. et al. Effects of quadriceps muscle fatigue on stiff-knee gait in patients with hemiparesis. *PloS One*. **9**, e94138 (2014).
16. Kerrigan, D. C., Gronley, J. & Perry, J. Stiff-legged gait in spastic paresis a study of quadriceps and hamstrings muscle activity. *Am. J. Phys. Med. Rehabil.* **70**, 294–305 (1991).
17. Francisco, G. E. & McGuire, J. R. Poststroke spasticity management. *Stroke* **43**, 3132–3136 (2012).
18. Simpson, D. et al. Assessment: Botulinum neurotoxin for the treatment of spasticity (an evidence-based review): [RETIRED] report of the therapeutics and technology assessment subcommittee of the American academy of neurology. *Neurology* **70**, 1691–1698 (2008).
19. Gracies, J. M. et al. Botulinum toxin Dilution and endplate targeting in spasticity: A double-blind controlled study. *Arch. Phys. Med. Rehabil.* **90**, 9–16 (2009). e12.
20. Van Campenhout, A., Verhaegen, A., Pans, S. & Molenaers, G. Botulinum toxin type A injections in the Psoas muscle of children with cerebral palsy: Muscle atrophy after motor end plate-targeted injections. *Res. Dev. Disabil.* **34**, 1052–1058 (2013).
21. Becker, I., Baxter, G. & Woodley, S. The vastus lateralis muscle: An anatomical investigation. *Clin. Anat.* **23**, 575–585 (2010).
22. Patil, S., Grigoris, P., Shaw-Dunn, J. & Reece, A. Innervation of vastus lateralis muscle. *Clin. Anat.: Off. J. Am. Assoc. Clin. Anatom. Br. Assoc. Clin. Anat.* **20**, 556–559 (2007).
23. Mu, L. & Sanders, I. Sihler's whole mount nerve staining technique: A review. *Biotech. Histochem.* **85**, 19–42 (2010).
24. Yi, K. H. et al. Intramuscular neural distribution of the vastus medialis for botulinum neurotoxin injection: Application to spasticity. *Surg. Radiol. Anat.* **46**, 2067–2073 (2024).
25. Page, B. J. et al. The relative location of the major femoral nerve motor branches in the thigh. *Cureus* **11** (2019).
26. Singh, R., Tubbs, S. & Singla, M. Classification and fascicular analysis of variant branching pattern of femoral nerve for microsurgical intervention. A series of thirteen cadavers. *Int. J. Morphol.* **34** (2016).
27. Patil, S., Grigoris, P., Shaw-Dunn, J. & Reece, A. T. Innervation of vastus lateralis muscle. *Clin. Anat.* **20**, 556–559 (2007).

28. Chan, S. L., Wong, M. & Tan, B. K. An anatomical and histological study of the vastus lateralis muscle nerve and application for functional muscle transfer in upper lip reconstruction. *J. Plast. Reconstr. Surg.* **1**, 44–51 (2022).
29. Betz, T. M., Wehrstein, M., Preisner, F., Bendszus, M. & Friedmann-Bette, B. Reliability and validity of a standardized ultrasound examination protocol to quantify vastus lateralis muscle. *J. Rehabil. Med.* **53**, 2809 (2021).
30. Franchi, M. V. et al. Muscle thickness correlates to muscle cross-sectional area in the assessment of strength training-induced hypertrophy. *Scand. J. Med. Sci. Sports*. **28**, 846–853 (2018).
31. Jacob, I., Johnson, M. I., Jones, G., Jones, A. & Francis, P. Age-related differences of vastus lateralis muscle morphology, contractile properties, upper body grip strength and lower extremity functional capability in healthy adults aged 18 to 70 years. *BMC Geriatr.* **22**, 538 (2022).
32. Piasecki, M. et al. Age-related neuromuscular changes affecting human vastus lateralis. *J. Physiol.* **594**, 4525–4536 (2016).
33. Pingel, J. et al. Injection of high dose botulinum-toxin A leads to impaired skeletal muscle function and damage of the fibrilar and non-fibrilar structures. *Sci. Rep.* **7**, 14746 (2017).
34. Li, Y. et al. Anatomical localization of nerve entry points and centers of intramuscular nerve dense region in quadriceps femoris and its significance in blocking muscle spasticity. *Int. J. Clin. Exp. Med.* **12**, 13981–13992 (2019).
35. Singer, B. J., Silbert, B. I., Silbert, P. L. & Singer, K. P. The role of botulinum toxin type A in the clinical management of refractory anterior knee pain. *Toxins* **7**, 3388–3404 (2015).
36. Monte, A. & Franchi, M. V. Regional muscle features and their association with knee extensors force production at a single joint angle. *Eur. J. Appl. Physiol.* **123**, 2239–2248 (2023).
37. Blazevich, A. J., Gill, N. D. & Zhou, S. Intra- and intermuscular variation in human quadriceps femoris architecture assessed in vivo. *J. Anat.* **209**, 289–310 (2006).

Acknowledgements
This study was conducted in compliance with the principles of the Declaration of Helsinki. Consent was obtained from the families of the deceased patients before beginning the dissection. The authors sincerely thank those who donated their bodies to science for anatomical research. The results of such research can potentially increase the overall knowledge of mankind, which can improve patient care. Therefore, these donors and their families deserve the greatest gratitude.

Author contributions
All authors have reviewed and approved the article for submission. Conceptualization, Kyu-Ho Yi, Ji-Hyun Lee, Hye-Won Hu Writing—Original Draft Preparation, Kyu-Ho Yi, Hye-Won Hu, Sung-Oh Hwang Writing—Review & Editing, Kyu-Ho Yi, Ji-Hyun Lee, Hyung-Jin Lee Visualization, Hyung-Jin Lee, Hye-Won Hu Supervision, Ji-Hyun Lee, Hyung-Jin Lee.

Funding
The authors declare that they have no financial interests related to the material of this manuscript.

Declarations

Competing interests
I acknowledge that I have considered the conflict of interest statement in the "Author Guidelines." To the best of my knowledge, I certify that no aspect of my current personal or professional situation might reasonably be expected to significantly affect my views on the subject I am presenting.The authors declare no competing interests.

Ethical approval
All cadavers involved were lawfully donated to the Surgical Anatomy Education Center at the Catholic University of Korea, College of Medicine, following approval by the Institutional Review Board (IRB approval code: Approval No. MC23EISE0022; approval date: March 24, 2023).

Additional information

Correspondence and requests for materials should be addressed to J.-H.L. or H.-J.L.